Journal of Alloys and Compounds 506 (2010) 565–568

Contents lists available at ScienceDirect

Journal of Alloys and Compounds

journal homepage: www.elsevier.com/locate/jallcom

Calorimetric investigations on cubic $BaTiO_3$ and $Ba_{0.9}Nd_{0.1}TiO_3$ systems

R. Babu[a], R. Kandan[a], Hrudananda Jena[b], K.V. Govindan Kutty[b], K. Nagarajan[a,*]

[a] Fuel Chemistry Division, Chemistry Group, Indira Gandhi Centre for Atomic Research, Kalpakkam 603 102, Tamilnadu, India
[b] Liquid Metals and Structural Chemistry Division, Chemistry Group, Indira Gandhi Centre for Atomic Research, Kalpakkam 603 102, Tamilnadu, India

ARTICLE INFO

Article history:
Received 20 May 2010
Received in revised form 2 July 2010
Accepted 9 July 2010
Available online 15 July 2010

Keywords:
Ceramic nuclear waste
Cubic barium titanate
Drop calorimetry
Heat capacity
Thermodynamic functions

ABSTRACT

Drop calorimetric studies were carried out on cubic $BaTiO_3$ and $Ba_{0.9}Nd_{0.1}TiO_3$. Enthalpy increments were measured by inverse drop calorimetric method in the temperature range 573–1523 K using a multidetector high temperature calorimeter. Thermodynamic functions such as heat capacity, entropy, Gibbs energy functions in the temperature range 298–1600 K were computed from the measured enthalpy increments.

1. Introduction

Ceramic nuclear waste forms such as synroc, tailored ceramics, TiO_2-matrix ceramics, glass ceramics and monazite, etc., which are alternative to glass, are under development. The TiO_2-matrix ceramics, an assemblage of geologically stable titanate minerals and its derivatives have been extensively considered as potential candidates for the immobilization of high level radioactive waste streams, since they are chemically more durable than the silicate assemblage due to their extremely low solubility [1–4]. Titanate ceramic formulations have evolved from the original polyphase assemblage to deal with the wide range of fission products, actinides, process chemicals and also more specific compositions of partitioned fission products or actinides. Alkaline earths and rare earths are the two major groups of fission product elements in the radioactive waste stream. A lanthanide fission product, neodymium, was chosen, in this study, to simulate the behaviour of its transuranium counterpart. The titanates formed by the alkaline earths, such as $BaTiO_3$ and $Ba_{1-x}Nd_xTiO_3$ are the probable phases in the waste matrix. In the selection of the nuclear waste forms, the thermodynamic stability of the constituent phases plays a vital role.

Barium titanate is also the most widely used dielectric material for application in multilayer capacitors. Pure and doped barium titanate ceramics also find application as potential candidates for intermediate-temperature fuel cell electrolytes, steam electrolysers, hydrogen and humidity sensors due to their proton conducting nature [5]. Hence the thermodynamic properties of $BaTiO_3$ and $Ba_{1-x}Nd_xTiO_3$ are of interest. Heat capacity measurements reported in the literature for $BaTiO_3$ are limited and data are available only at temperatures below 450 K [6–10]. For the neodymium-doped $BaTiO_3$, no data are available. Hence enthalpy increment measurements were carried out on $BaTiO_3$ and $Ba_{0.9}Nd_{0.1}TiO_3$, having cubic crystal structures, in the temperature range 573–1523 K by drop calorimetry, using a multidetector high temperature drop calorimeter. $BaTiO_3$ usually crystallizes in the tetragonal system, but in the present case, pristine and Nd-doped $BaTiO_3$ could be stabilized in the cubic system by employing innovative methods of materials synthesis. The thermodynamic functions of the cubic phases are reported here for the first time.

2. Experimental

2.1. Preparation and characterization

$BaTiO_3$ was prepared in the form of fine powder by gel to crystallite conversion technique and hydrothermal method, as reported in detail elsewhere [11,12]. In both the methods for the preparation $BaTiO_3$, the starting materials, $Ba(OH)_2$ and $TiOCl_2$ were taken in such a way that the starting stoichiometry of barium and titanium are in the ratio of 1.05:1.0. The hydrated gels of $TiO_2{\cdot}xH_2O$ were precipitated out from dilute aqueous solutions of $TiOCl_2$. The gel was washed with boiled distilled water to make it free from chloride and ammonia. The gel was transferred to a Teflon container having a tight lid and weighed amount of $Ba(OH)_2{\cdot}8H_2O$ was added to it. The Teflon container was kept inside an autoclave and heated at 415 K for 4 h. The powders formed were washed thoroughly with boiled distilled water (CO_2-free) till the powder was free from unreacted $Ba(OH)_2$. The oven-dried (373 K) powders were examined by X-ray powder diffraction using CuK_α radiation, employing a Siemens D-500 powder X-ray diffractometer, in the step scan mode with a step size of 0.02°

---

* Corresponding author. Tel.: +91 44 27480500x24289; fax: +91 44 27480065.
E-mail address: knag@igcar.gov.in (K. Nagarajan).

0925-8388/$ – see front matter © 2010 Elsevier B.V. All rights reserved.
doi:10.1016/j.jallcom.2010.07.077

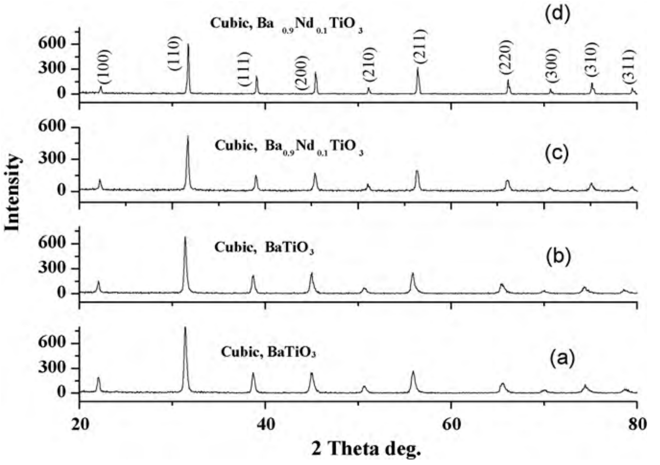

Fig. 1. XRD patterns of pure and Nd-doped $BaTiO_3$: (a) and (c) As-prepared samples; (b) and (d) after enthalpy increment measurements.

2θ/s and a counting time of 2 s per step. A similar procedure was adopted for the preparation and characterization of $Ba_{0.9}Nd_{0.1}TiO_3$. $BaTiO_3$ and $Ba_{0.9}Nd_{0.1}TiO_3$ synthesized by hydrothermal and gel to crystallite conversion methods were seen to be single phase materials with cubic symmetry ($a = 4.03 \pm 0.01$ Å for $BaTiO_3$ and $a = 4.01 \pm 0.01$ Å for $Ba_{0.9}Nd_{0.1}TiO_3$) as revealed by XRD. The XRD patterns of the as-prepared samples and that of the samples after calorimetric measurements are shown in Fig. 1, and there is no phase transformation in the temperature range of measurement.

2.2. *Multi-detector high temperature calorimeter*

The enthalpy increments of the titanates were determined by drop calorimetry using SETARAM multi-detector high temperature calorimeter (MHTC-96). The calorimetric detector is a thermopile comprising 28 thermocouples embedded on the inner side of an alumina tube in which the sample crucible and an empty reference crucible are positioned one above the other. In the thermopile detector, the thermocouples are positioned at heights surrounding the outer surfaces of the crucibles so that an integrated heat exchange between the two crucibles is obtained at the output signal. In the present study, a detector, made up of Pt–30%Rh/Pt–10% thermocouples was employed. The detector is centered in a gas-tight alumina muffle placed in the furnace heated by a single graphite resistance element. All measurements were performed in ultra high pure argon atmosphere.

2.3. *Enthalpy increment measurements*

In a typical experiment, carried out at a constant temperature four or five titanate sample pellets and an equal number of α-alumina reference (SRM 720) pellets each weighing about 150–200 mg, were dropped one after the other from the specimen chamber maintained at the ambient temperature into the sample crucible kept in the calorimeter maintained at a constant temperature T. From the resultant heat flow signals corresponding to the α-alumina reference (Q_R) and the titanate sample (Q_S), the enthalpy increments of the titanate samples $(H_T - H_{298})_S$ were computed using the known enthalpy increment values of α-alumina reference $(H_T - H_{298})_R$ from the literature [13] and the following expression:

$$(H_T - H_{298})_S = \frac{\int Q_S dt}{\int Q_R dt} \cdot \frac{M_S}{m_S} \cdot \frac{m_R}{M_R} \cdot (H_T - H_{298})_R$$

where M_R and m_R are the molar mass and mass of the α-alumina reference material and M_S and m_S are the molar mass and mass of the titanate sample. The mean of the five heat flow values for the standard and that for the sample were used to compute the enthalpy increment at that temperature, T. Further, four or five measurements were carried out for a given temperature and the mean value of the enthalpy increments from these runs at temperature, T were used for fitting.

Table 1
Enthalpy increments of $BaTiO_3$.

T (K)	$H_T - H_{298}$ (kJ mol^{-1})	
	Experimental	Calculated from Eq. (1)
573	34.901	32.321
623	39.993	38.697
673	45.455	45.157
723	55.112	51.690
773	60.004	58.289
823	64.850	64.946
873	70.128	71.657
923	76.920	78.418
973	86.050	85.226
1023	92.136	92.078
1073	97.846	98.973
1123	106.609	105.909
1173	112.103	112.884
1223	116.386	119.898
1273	123.899	126.949
1323	136.170	134.037
1373	139.236	141.161
1423	153.076	148.320

Table 2
Enthalpy increments of $Ba_{0.9}Nd_{0.1}TiO_3$.

T (K)	$H_T - H_{298}$ (kJ mol^{-1})	
	Experimental	Calculated from Eq. (2)
573	37.330	32.607
623	42.661	39.054
673	47.347	45.594
723	54.390	52.215
773	60.404	58.909
823	67.318	65.671
873	71.782	72.494
923	76.910	79.376
973	87.553	86.313
1023	92.099	93.304
1073	97.035	100.346
1123	103.633	107.438
1173	114.355	114.579
1223	121.611	121.766
1273	128.896	129.000
1323	136.211	136.280
1373	143.556	143.605
1423	150.930	150.973
1473	159.904	158.386
1523	167.287	165.842

3. Results and discussion

The accuracy of the enthalpy increments from our measurements had been determined to be 2–4%. Enthalpy increments of $BaTiO_3$ and $Ba_{0.9}Nd_{0.1}TiO_3$ were measured in the temperature ranges of 573–1423 K and 573–1523 K, respectively. They were fitted to polynomial functions in temperature by the least squares method using the following two constraints: (i) $(H_T - H_{298}) = 0$ at 298 K; (ii) the derivative of the function at 298 K is equal to the value of heat capacity at 298 K. The $C_{p,298}$ values for the $BaTiO_3$ and $Ba_{0.9}Nd_{0.1}TiO_3$ (which were estimated from $C^0_{p,298}$ of its constituent oxides from the literature [14] by invoking molar additivity rule to be 101.87 and 102.76 J K^{-1} mol^{-1}, respectively). Similarly the S^0_{298} value of $BaTiO_3$ and S_{298} value of $Ba_{0.9}Nd_{0.1}TiO_3$ needed for computing entropy and Gibbs energy functions were also estimated from the entropy values of constituent oxides [14]. However, for the estimation of S_{298} value $Ba_{0.9}Nd_{0.1}TiO_3$ the contribution of ideal entropy of mixing was taken into consideration. The fit equations thus obtained for $BaTiO_3$ and $Ba_{0.9}Nd_{0.1}TiO_3$ are given below:

$BaTiO_3$

$$(H_T - H_{298}) = 127.561T + 6.064 \times 10^{-3}T^2 + 26.052 \times 10^5 T^{-1} - 47,309 \qquad (1)$$

$Ba_{0.9}Nd_{0.1}TiO_3$

$$(H_T - H_{298}) = 126.636T + 7.883 \times 10^{-3}T^2 + 25.403 \times 10^5 T^{-1} - 46,978 \qquad (2)$$

Table 3
Thermodynamic functions of $BaTiO_3$ calculated from Eq. (1).

T (K)	$H_T - H_{298}$ (kJ mol^{-1})	C_P (J K^{-1} mol^{-1})	S_T (J K^{-1} mol^{-1})	$-(G_T - H_{298})/T$ (J K^{-1} mol^{-1})
298	0	101.87	122.70	122.70
300	0.189	102.25	123.33	122.70
400	11.198	116.13	154.90	126.91
500	23.198	123.20	181.65	135.26
600	35.752	127.60	204.53	144.94
700	48.677	130.73	224.45	154.91
800	61.877	133.19	242.07	164.72
900	75.302	135.26	257.88	174.21
1000	88.921	137.08	272.23	183.30
1100	102.714	138.75	285.37	191.99
1200	116.667	140.31	297.51	200.29
1300	130.772	141.79	308.80	208.21
1400	145.022	143.21	319.36	215.77
1500	159.413	144.60	329.29	223.01
1600	173.940	145.95	338.66	229.95

Table 4
Thermodynamic functions of $Ba_{0.9}Nd_{0.1}TiO_3$ calculated from Eq. (2).

T (K)	$H_T - H_{298}$ (kJ mol^{-1})	C_P (J K^{-1} mol^{-1})	S_T (J K^{-1} mol^{-1})	$-(G_T - H_{298})/T$ (J K^{-1} mol^{-1})
298	0	102.76	120.72	120.72
300	0.190	103.14	121.36	120.72
400	11.289	117.17	153.19	124.97
500	23.392	124.36	180.17	133.38
600	36.076	129.04	203.28	143.15
700	49.159	132.49	223.41	153.21
800	62.552	135.28	241.32	163.13
900	76.203	137.69	257.40	172.73
1000	90.082	139.86	272.02	181.94
1100	104.170	141.88	285.44	190.74
1200	118.454	143.79	297.87	199.16
1300	132.926	145.63	309.45	207.20
1400	147.578	147.41	320.31	214.90
1500	162.407	149.16	330.54	222.27
1600	177.408	150.87	340.22	229.34

In the above equations, the temperature is expressed in K and the enthalpy increment in J mol^{-1}. The standard errors of the fit are 2.7% and 2.4% and the estimates of the standard deviations for the fit are 2438 J mol^{-1} and 2339 J mol^{-1} for $BaTiO_3$ and $Ba_{0.9}Nd_{0.1}TiO_3$, respectively. The experimental values of the enthalpy increments of $BaTiO_3$ and $Ba_{0.9}Nd_{0.1}TiO_3$ are given in Tables 1 and 2 along with the calculated values from Eqs. (1) and (2). From the above fit equations, heat capacity, entropy and Gibbs energy function have also been computed which are given in Tables 3 and 4. The measured enthalpy increment values of $BaTiO_3$ and $Ba_{0.9}Nd_{0.1}TiO_3$ are shown in Fig. 2 along with the fit values as well as those computed using molar additivity rule from the enthalpy data of the component oxides from the literature [13]. The values from the fit are within ±3% of the measured values. Present enthalpy increment data are in agreement within 4% with the mole average values calculated for $BaTiO_3$ and $Ba_{0.9}Nd_{0.1}TiO_3$. Fig. 3 shows the present heat capacity data for $BaTiO_3$ and $Ba_{0.9}Nd_{0.1}TiO_3$ along with the heat capacity data computed from the literature by using the molar

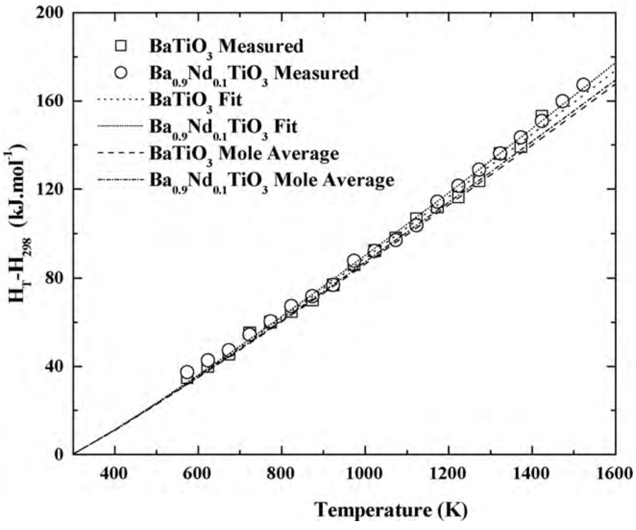

Fig. 2. Enthalpy increments of pure and Nd-doped $BaTiO_3$.

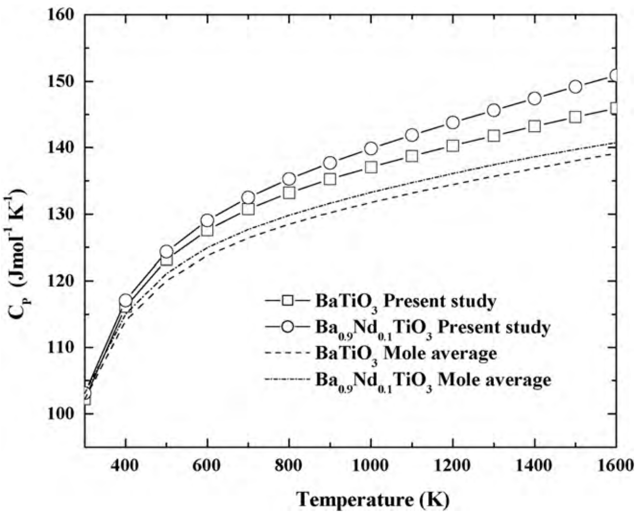

Fig. 3. Heat capacity of pure and Nd-doped $BaTiO_3$.

additivity rule. As can be seen from Fig. 3, the present heat capacity data are higher than the mole average values. The deviations are about 4 and 5% for pure $BaTiO_3$ and $Ba_{0.9}Nd_{0.1}TiO_3$ at 1000 K and they increase with increase in temperature. The larger deviation at higher temperatures could be due to the contribution of anharmonicity.

4. Conclusion

Enthalpy increments of $BaTiO_3$ and $Ba_{0.9}Nd_{0.1}TiO_3$ having cubic crystal structures have been measured in the temperature ranges 573–1523 K for the first time by inverse drop calorimetry. Other thermodynamic functions, namely, heat capacity, entropy and Gibbs energy functions were computed in the temperature range 298–1600 K.

References

[1] W. Lutze, R.C. Ewing, Radioactive Waste Forms for the Future, North-Holland, Amsterdam, 1988.

[2] G.J. McCarthy, W.B. White, R. Roy, B.E. Scheetz, S. Komarneni, D.K. Smith, D.M. Roy, Nature 273 (1978) 216–217.

[3] G.R. Lumpkin, K.L. Smith, M.G. Blackford, J. Nucl. Mater. 224 (1995) 31–42.

[4] K.L. Smith, G.R. Lumpkin, M.G. Blackford, R.A. Day, K.P. Hart, J. Nucl. Mater. 190 (1992) 287–294.

[5] H. Jena, V.K. Mittal, S. Bera, S.V. Narasimhan, K.V. Govindan Kutty, T.R.N. Kutty, Appl. Surf. Sci. 254 (2008) 7074–7079.

[6] I. Hatta, A. Ikushima, J. Phys. Soc. Jpn. 41 (2) (1976) 558–564.

[7] Y. Akishige, T. Atake, Y. Saito, E. Sawaguchi, J. Phys. Soc. Jpn. 57 (3) (1988) 718–721.

[8] Y. He, Thermochim. Acta 419 (2004) 135–141.

[9] F. Baeten, B. Derks, W. Coppens, V. Kleef, J. Eur. Cer. Soc. 26 (2006) 589–592.

[10] K. Morimoto, S. Sawai, K. Hisano, T. Yamamoto, Thermochim. Acta 442 (2006) 14–17.

[11] P. Padmini, T.R.N. Kutty, J. Mater. Chem. 4 (1994) 1875–1881.

[12] H. Jena, K.V.G. Kutty, T.R.N. Kutty, Mater. Res. Bull. 39 (2004) 489–511.

[13] Synthetic Sapphire Al_2O_3, Certificate of Standard Reference Materials 720, National Bureau of Standards, U.S. Department of Commerce, Washington, DC 20234, USA, 1982, https://www-s.nist.gov/srmors/certificates/720.pdf?CFID.

[14] O. Kubaschewski, C.B. Alcock, P.J. Spencer, Metallurgical Thermochemistry, 6th edition, Pergamon Press, Oxford, 1993.